
Robust Matrix Factorization with Grouping Effect

Haiyan Jiang¹, Shuyu Li^{2†}, Luwei Zhang^{2†}, Haoyi Xiong¹, Dejing Dou¹

¹ Baidu Research, Baidu Inc., China

² Columbia University, New York, NY, USA

jianghaiyan01@baidu.com,
shuryli@outlook.com, helenzhang0322@gmail.com,
xionghaoyi@baidu.com, doudejing@baidu.com

Abstract

Although many techniques have been applied to matrix factorization (MF), they may not fully exploit the feature structure. In this paper, we incorporate the grouping effect into MF and propose a novel method called *Robust Matrix Factorization with Grouping effect* (GRMF). The grouping effect is a generalization of the sparsity effect, which conducts denoising by clustering similar values around multiple centers instead of just around 0. Compared with existing algorithms, the proposed GRMF can automatically learn the grouping structure and sparsity in MF without prior knowledge, by introducing a naturally adjustable non-convex regularization to achieve simultaneous sparsity and grouping effect. Specifically, GRMF uses an efficient alternating minimization framework to perform MF, in which the original non-convex problem is first converted into a convex problem through Difference-of-Convex (DC) programming, and then solved by Alternating Direction Method of Multipliers (ADMM). In addition, GRMF can be easily extended to the Non-negative Matrix Factorization (NMF) settings. Extensive experiments have been conducted using real-world data sets with outliers and contaminated noise, where the experimental results show that GRMF has promoted performance and robustness, compared to five benchmark algorithms.

Keywords: Robust Matrix Factorization, Feature Grouping, Sparsity, Non-convex Regularization

1 Introduction

Matrix factorization (MF) is a fundamental yet widely-used technique in machine learning (Chi et al., 2019, Choi, 2008, Dai et al., 2020, Li et al., 2019, Mnih and Salakhutdinov, 2007, Parvin et al., 2019, Srebro et al., 2005, Wang et al., 2020), with numerous applications in computer vision (Gao et al., 2022, Haeffele and Vidal, 2019, Wang and Yeung, 2013, Wang et al., 2012, Xu et al., 2020), recommender systems (Jakomin et al., 2020, Koren et al., 2009, Xue et al., 2017), bioinformatics (Cui et al., 2019, Gaujoux and Seoighe, 2010, Jamali et al., 2020, Pascual-Montano et al., 2006), social networks (Gurini et al., 2018, Ma et al., 2008, Zhang et al., 2020), and many others. In MF, with a given data matrix $\mathbf{Y} \in \mathbb{R}^{d \times n}$, one is interested in approximating \mathbf{Y} by \mathbf{UV}^T such that the reconstruction error between the given matrix and its factorization is minimized, where $\mathbf{U} \in \mathbb{R}^{d \times r}$, $\mathbf{V} \in \mathbb{R}^{n \times r}$, and $r \ll \min(d, n)$ is the rank. Various regularizers have been introduced to generalize the low-rank MF under different conditions and constraints in the following form

$$\min_{\mathbf{U} \in \mathbb{R}^{d \times r}, \mathbf{V} \in \mathbb{R}^{n \times r}} \frac{1}{2} \|\mathbf{Y} - \mathbf{UV}^T\|_{\alpha}^{\alpha} + \mathcal{R}_1(\mathbf{U}) + \mathcal{R}_2(\mathbf{V}), \quad (1.1)$$

[†]The work was done when the author was an intern at Baidu Research.

where \mathcal{R}_1 and \mathcal{R}_2 refer to the regularization terms and α corresponds to the loss types (e.g., $\alpha = 2$ for the quadratic loss) for reconstruction errors. Existing studies (Abdolali and Gillis, 2021, Kim et al., 2012, Lin et al., 2017) show that the use of regularization terms could prevent overfitting or impose sparsity, while the choice of loss types (e.g., $\alpha = 1$ for ℓ_1 -loss) helps to establish robustness of MF with outliers and noise.

Background The goal of matrix factorization is to obtain the low-dimensional structures of the data matrix while preserving the major information, where singular value decomposition (SVD) (Klema and Laub, 1980) and principal component analysis (PCA) (Wold et al., 1987) are two conventional solutions. To better deal with sparsity in high-dimensional data, the truncated-SVD (Hansen, 1987) is proposed to achieve result with a determined rank. Like traditional SVD, it uses the ℓ_2 loss for reconstruction errors, but has additional requirement on the norm of the solution.

Loss terms in MF While the above models could partially meet the goal of MF, they might be vulnerable to outliers and noise and lack robustness. Thus they often give unsatisfactory results on real world data due to the use of inappropriate loss terms for reconstruction errors. To solve the problem, Wang et al. (2012) proposed a probabilistic method for robust matrix factorization (PRMF) based on the ℓ_1 loss which is formulated using the Laplace error assumption and optimized with a parallelizable Expectation-Maximization (EM) algorithm. In addition to traditional ℓ_1 or ℓ_2 -loss, researchers have also made attempts with non-convex loss functions. Yao and Kwok (2018) constructed a scalable robust matrix factorization with non-convex loss, using general non-convex loss functions to make the MF model applicable in more situations. On the contrary, Haeffele et al. (2014) employed the non-convex projective tensor norm. Yet another algorithm with identifiability guarantee has been proposed in Abdolali and Gillis (2021), where the simplex-structured matrix factorization (SSMF) is invented to constrain the matrix \mathbf{V} to belong to the unit simplex.

Sparsity control in MF In addition to the loss terms, sparsity regularizers or constraints have been proposed to control the number of nonzero elements in MF (either the recovered matrix or the noise matrix). For example, Hoyer (2004) employed a sparseness measure based on the relationship between the ℓ_1 -norm and the ℓ_2 -norm. Candès et al. (2011) introduced a Robust PCA (RPCA) which decomposes the matrix M by $M = L_0 + S_0$, where L_0 is assumed to have low-rank and S_0 is constrained to be sparse by an ℓ_1 regularizer. The Robust Non-negative Matrix Factorization (RNMF) (Zhang et al., 2011) decomposes the non-negative data matrix as the summation of one sparse error matrix and the product of two non-negative matrices, where the sparsity of the error matrix is constrained with ℓ_1 -norm penalty. Compared with the ℓ_2 -norm penalty and the ℓ_1 -norm penalty used in the mentioned methods, the ℓ_0 -norm penalty directly addresses the sparsity measure. However, the direct use of the ℓ_0 -norm penalty gives us a non-convex NP-hard optimization problem. To address that difficulty, researchers have proposed different approximations, such as the truncated ℓ_1 penalty proposed in Shen et al. (2012).

Our work Previous studies on MF pay great attention to sparsity, yet few of them (Li et al., 2013, Ortega et al., 2016, Rahimpour et al., 2017, Yuen et al., 2012) take care of the grouping effect. While sparse control can only identify factors whose weights are clustered around 0 and eliminate the noise caused by them, the grouping effect can identify factor groups whose weights are clustered around any similar value and eliminate the noise caused by all these groups. In fact, the grouping effect can bring interpretability and recovery accuracy to MFs to a larger extent than sparsity alone does. With the desire to conduct matrix factorization with robustness, sparsity, and grouping effect, we construct a new matrix factorization model named *Robust Matrix Factorization with Grouping effect* (GRMF) and evaluate its performance through experiments.

To the best of our knowledge, this work has made unique contributions in introducing sparsity and grouping effect into MF. The most relevant works are Kim et al. (2012), Yang et al. (2012). Specifically, Shen et al. (2012), Yang et al. (2012) proposed to use truncated ℓ_1 penalty to pursue both sparsity and grouping effect in estimation of linear regression models, while the way of using such techniques to improve MF is not known. On the other hand, Kim et al. (2012) also modeled MF with groups but assumes features in the same group sharing the same sparsity pattern with predefined group partition. Thus a mixed norm regularization is proposed to promote group sparsity in the factor matrices of non-negative MF. Compared to Kim et al. (2012), our proposed GRMF is more general-purpose, where the sparsity (e.g., elements in the factor matrix centered around zero) is only one special group in all possible groups for elements in factor matrices.

Specifically, to achieve robustness, the focus of GRMF is on matrix factorization under the ℓ_1 -loss. GRMF further adopts an ℓ_0 surrogate—truncated ℓ_1 , for the penalty term to control the sparsity and the grouping effect. As the resulting problem is non-convex, we solve it with difference-of-convex algorithm (DC) and Alternating Direction Method of Multipliers (ADMM). The algorithms are implemented to conduct experiments on COIL-20, ORL, extended Yale B, and JAFFE datasets. In addition, we compare the result with 5 benchmark algorithms: Truncated SVD (Hansen, 1987), RPCA (Candès et al., 2011), RNMF (Wen et al., 2018), RPMF (Wang et al., 2012) and GoDec+ (Guo et al., 2017). The results show that the proposed GRMF significantly outperforms existing benchmark algorithms.

The remainder of the paper is organized as follows. In Section 2, we briefly introduce the robust MF and the non-negative MF. We propose the GRMF in Section 3 and give the algorithm for GRMF which uses DC and ADMM for solving the resulting non-convex optimization problem in Section 4. Experiment results to show the performances of GRMF and comparison with other benchmark algorithms are presented in Section 5. We conclude the paper in Section 6.

Notations For a scalar x , $\text{sign}(x) = 1$ if $x > 0$, 0 if $x = 0$, and -1 otherwise. For a matrix \mathbf{A} , $\|\mathbf{A}\|_F = (\sum_{i,j} A_{ij}^2)^{\frac{1}{2}}$ is its Frobenius norm, and $\|\mathbf{A}\|_{\ell_1} = \sum_{i,j} |A_{ij}|$ is its ℓ_1 -norm. For a vector \mathbf{x} , $\|\mathbf{x}\|_{\ell_1} = \sum_i |x_i|$ is its ℓ_1 -norm. Denote data matrix $\mathbf{Y}_{d \times n} = [\mathbf{y}_{\cdot 1}, \dots, \mathbf{y}_{\cdot n}]$ the stack of n column vectors with each $\mathbf{y}_{\cdot j} \in \mathbb{R}^d$, or $\mathbf{Y}^T = [\mathbf{y}_1^T, \dots, \mathbf{y}_n^T]$ the stack of d row vectors with each $\mathbf{y}_i \in \mathbb{R}^n$. Denote $\mathbf{U}^T = [\mathbf{u}_1, \dots, \mathbf{u}_d] \in \mathbb{R}^{r \times d}$, and $\mathbf{V}^T = [\mathbf{v}_1, \dots, \mathbf{v}_n] \in \mathbb{R}^{r \times n}$, with each $\mathbf{u}_1, \dots, \mathbf{u}_d, \mathbf{v}_1, \dots, \mathbf{v}_n \in \mathbb{R}^r$. Denote \mathbf{v}_{jl} the l -th element of the vector $\mathbf{v}_j \in \mathbb{R}^r$ and \mathbf{u}_{il} the l -th element of the vector $\mathbf{u}_i \in \mathbb{R}^r$.

2 Preliminaries

Robust matrix factorization (RMF) Given a data matrix $\mathbf{Y} \in \mathbb{R}^{d \times n}$, the matrix factorization (Yao and Kwok, 2018) is formulated as $\mathbf{Y} = \mathbf{U}\mathbf{V}^T + \varepsilon$. Here $\mathbf{U} \in \mathbb{R}^{d \times r}$, $\mathbf{V} \in \mathbb{R}^{n \times r}$, $r \ll \min(d, n)$ is the rank, and ε is the noise/error term. The RMF can be formulated under the Laplacian error assumption, $\min_{\mathbf{U}, \mathbf{V}} \|\mathbf{Y} - \mathbf{U}\mathbf{V}^T\|_{\ell_1} = \sum_{i=1}^d \sum_{j=1}^n |y_{ij} - \mathbf{u}_i^T \mathbf{v}_j|$, where $\mathbf{U}^T = [\mathbf{u}_1, \dots, \mathbf{u}_d] \in \mathbb{R}^{r \times d}$, and $\mathbf{V}^T = [\mathbf{v}_1, \dots, \mathbf{v}_n] \in \mathbb{R}^{r \times n}$. Adding regularizers gives the optimization problem, $\min_{\mathbf{U} \in \mathbb{R}^{d \times r}, \mathbf{V} \in \mathbb{R}^{n \times r}} \|\mathbf{Y} - \mathbf{U}\mathbf{V}^T\|_{\ell_1} + \frac{\lambda_u}{2} \|\mathbf{U}\|_2^2 + \frac{\lambda_v}{2} \|\mathbf{V}\|_2^2$.

Robust non-negative matrix factorization (RNMF) As the traditional NMF is optimized under the Gaussian noise or Poisson noise assumption, RNMF (Zhang et al., 2011) is introduced to deal with data that are grossly corrupted. RNMF decomposes the non-negative data matrix as the summation of one sparse error matrix and the product of two non-negative matrices. The formulation states $\min_{\mathbf{W}, \mathbf{H}, \mathbf{S}} \|\mathbf{Y} - \mathbf{W}\mathbf{H} - \mathbf{S}\|_F^2 + \lambda \|\mathbf{S}\|_{\ell_1}$ s.t. $\mathbf{W} \geq 0, \mathbf{H} \geq 0$, where $\|\cdot\|_F$ is the Frobenius norm, $\|\mathbf{S}\|_{\ell_1} = \sum_{i=1}^d \sum_{j=1}^n |S_{ij}|$, and $\lambda > 0$ is the regularization parameter, controlling the sparsity of \mathbf{S} .

3 Proposed GRMF formulation

In this section, we introduce our *Robust Matrix Factorization with Grouping effect* (GRMF) by incorporating the grouping effect into MF. The problem of GRMF is formulated as follows

$$\min_{\mathbf{U} \in \mathbb{R}^{d \times r}, \mathbf{V} \in \mathbb{R}^{n \times r}} f(\mathbf{U}, \mathbf{V}) = \|\mathbf{Y} - \mathbf{U}\mathbf{V}^T\|_{\ell_1} + \mathcal{R}(\mathbf{U}) + \mathcal{R}(\mathbf{V}), \quad (3.1)$$

where $\mathcal{R}(\mathbf{U})$ and $\mathcal{R}(\mathbf{V})$ are two regularizers corresponding to \mathbf{U} and \mathbf{V} , given by

$$\begin{aligned} \mathcal{R}(\mathbf{U}) &= \sum_{i=1}^d \lambda_1 \mathcal{P}_1(\mathbf{u}_i) + \sum_{i=1}^d \lambda_2 \mathcal{P}_2(\mathbf{u}_i) + \sum_{i=1}^d \lambda_3 \mathcal{P}_3(\mathbf{u}_i), \text{ and} \\ \mathcal{R}(\mathbf{V}) &= \sum_{j=1}^n \lambda_1 \mathcal{P}_1(\mathbf{v}_j) + \sum_{j=1}^n \lambda_2 \mathcal{P}_2(\mathbf{v}_j) + \sum_{j=1}^n \lambda_3 \mathcal{P}_3(\mathbf{v}_j). \end{aligned}$$

Here $\mathcal{P}_1(\cdot)$, $\mathcal{P}_2(\cdot)$ and $\mathcal{P}_3(\cdot)$ are different penalty functions, which take the following form with respect to a vector $\mathbf{x} \in \mathbb{R}^r$,

$$\mathcal{P}_1(\mathbf{x}) = \sum_{l=1}^r \min\left(\frac{|x_l|}{\tau_1}, 1\right), \mathcal{P}_2(\mathbf{x}) = \sum_{l < l': (l, l') \in \mathcal{E}} \min\left(\frac{|x_l - x_{l'}|}{\tau_2}, 1\right), \mathcal{P}_3(\mathbf{x}) = \sum_{l=1}^r x_l^2, \quad (3.2)$$

where $\mathcal{P}_1(\cdot)$ and $\mathcal{P}_2(\cdot)$ are two regularization terms controlling the sparsity (feature selection) and the grouping effect (feature grouping), τ_1 and τ_2 are thresholding parameters asserting when a small weight or a small difference between two weights will be penalized, λ_1 and λ_2 are the corresponding tuning parameters. Here $\mathcal{P}_3(\cdot)$ is an inherited penalty term from MF with its tuning parameter λ_3 . The truncated ℓ_1 -norm penalty $\mathcal{P}_1(\cdot)$ can be viewed as a surrogate of the ℓ_0 -norm penalty for feature selection (Shen et al., 2012), where $\min(|x_l|/\tau, 1)$ is an approximation of $I(x_l \neq 0)$ when $\tau \rightarrow 0$. In addition, GRMF can be extended to non-negative MF (see details in Appendix B). For other notations, denote $\mathcal{E} = \{(l, l') : l \neq l', l, l' = 1, \dots, r\}$ a set of edges between two distinct nodes $l \neq l'$ of an undirected complete graph.

In the proposed GRMF, we adopt the ℓ_1 -loss to attain the robustness and introduce a naturally adjustable non-convex regularization to achieve simultaneous sparsity and grouping effect. Due to the non-convex regularization and the low-rank constraint in MF, the GRMF is a non-convex problem. By fixing \mathbf{U} or \mathbf{V} and updating the other one, GRMF becomes solvable.

4 Algorithms for GRMF

The GRMF problem includes the optimization of two matrices \mathbf{U} and \mathbf{V} , which are treated as two independent variables in the alternative optimization process, while the other is fixed.

Note that

$$\|\mathbf{Y} - \mathbf{U}\mathbf{V}^T\|_{\ell_1} = \sum_{j=1}^n \|\mathbf{y}_{\cdot j} - \mathbf{U}\mathbf{v}_j\|_{\ell_1} = \sum_{i=1}^d \|\mathbf{y}_i - \mathbf{V}\mathbf{u}_i\|_{\ell_1}.$$

During the alternative optimization procedure, \mathbf{U} and \mathbf{V} should be updated alternatively according to $L(\mathbf{U}|\mathbf{V})$ and $L(\mathbf{V}|\mathbf{U})$, which are given by

$$\min_{\mathbf{U} \in \mathbb{R}^{d \times r}} L(\mathbf{U}|\mathbf{V}) = \sum_{i=1}^d \|\mathbf{y}_i - \mathbf{V}\mathbf{u}_i\|_{\ell_1} + \sum_{i=1}^d \lambda_1 \mathcal{P}_1(\mathbf{u}_i) + \sum_{i=1}^d \lambda_2 \mathcal{P}_2(\mathbf{u}_i) + \sum_{i=1}^d \lambda_3 \mathcal{P}_3(\mathbf{u}_i), \quad (4.1)$$

$$\min_{\mathbf{V} \in \mathbb{R}^{n \times r}} L(\mathbf{V}|\mathbf{U}) = \sum_{j=1}^n \|\mathbf{y}_{\cdot j} - \mathbf{U}\mathbf{v}_j\|_{\ell_1} + \sum_{j=1}^n \lambda_1 \mathcal{P}_1(\mathbf{v}_j) + \sum_{j=1}^n \lambda_2 \mathcal{P}_2(\mathbf{v}_j) + \sum_{j=1}^n \lambda_3 \mathcal{P}_3(\mathbf{v}_j). \quad (4.2)$$

Note that the optimization problem of $L(\mathbf{U}|\mathbf{V})$ can be decomposed into d independent subproblems. The same procedure applies to the minimization of $L(\mathbf{V}|\mathbf{U})$. Thus, the problem of GRMF is a combination of $n + d$ optimization subproblems, each with respect to a vector in \mathbb{R}^r . For each subproblem, we use the difference-of-convex algorithm (DC) to approximate a non-convex cost function. At each iteration, a quadratic problem with equality constraints is solved by the Alternating Direction Method of Multipliers (ADMM).

The algorithm for GRMF consists of three steps. *First*, we apply an alternative minimization framework to decompose the problem of GRMF into $d + n$ independent subproblems, each optimizing \mathbf{v}_j (a column in \mathbf{V}^T) or \mathbf{u}_i (a column in \mathbf{U}^T). *Second*, the non-convex regularization function in each subproblem is decomposed into a difference of two convex functions, and, through linearizing

the trailing convex function, a sequence of approximations is constructed by its affine minorization. *Third*, the constructed quadratic problem with equality constraints is solved by ADMM.

Algorithm 1: The alternating minimization algorithm for GRMF

Input: Initialization $\mathbf{U}^{(0)}, \mathbf{V}^{(0)}$; tuning parameters $\lambda_1, \lambda_2, \lambda_3, \tau_1, \tau_2$; small tolerance $\delta_{\mathbf{U}}, \delta_{\mathbf{V}}$,
 $t = 1$.

Result: Optimal \mathbf{U}, \mathbf{V} .

while $\|\mathbf{U}^{(t)} - \mathbf{U}^{(t-1)}\|_F^2 < \delta_{\mathbf{U}}$ or $\|\mathbf{V}^{(t)} - \mathbf{V}^{(t-1)}\|_F^2 < \delta_{\mathbf{V}}$ **do**
 for $j = 1, \dots, n$ **do**
 | Update $\mathbf{v}_j^{(t)} = \arg \min_{\mathbf{v}_j \in \mathbb{R}^r} L(\mathbf{v}_j | \mathbf{U}^{(t-1)})$ by Algorithm 2;
 end
 Then update $[\mathbf{V}^{(t)}]^T = [\mathbf{v}_1^{(t)}, \dots, \mathbf{v}_n^{(t)}]$;
 for $i = 1, \dots, d$ **do**
 | Update $\mathbf{u}_i^{(t)} = \arg \min_{\mathbf{u}_i \in \mathbb{R}^r} L(\mathbf{u}_i | \mathbf{V}^{(t)})$ by Algorithm 2;
 end
 Then update $[\mathbf{U}^{(t)}]^T = [\mathbf{u}_1^{(t)}, \dots, \mathbf{u}_d^{(t)}]$;
 $t \leftarrow t + 1$;
end

4.1 Alternative minimization framework for GRMF

To solve the GRMF problem, we alternatively update $\mathbf{V}^T = [\mathbf{v}_1, \dots, \mathbf{v}_n] \in \mathbb{R}^{r \times n}$ (while fixing \mathbf{U}) and $\mathbf{U}^T = [\mathbf{u}_1, \dots, \mathbf{u}_d] \in \mathbb{R}^{r \times d}$ (while fixing \mathbf{V}). Thus the alternative minimization framework at the t -th step consists of updating $\mathbf{U}^{(t)} = \arg \min_{\mathbf{U}} L(\mathbf{U} | \mathbf{V}^{(t)})$ and $\mathbf{V}^{(t)} = \arg \min_{\mathbf{V}} L(\mathbf{V} | \mathbf{U}^{(t-1)})$ iteratively until convergence. Problem (4.1) is therefore decomposed into d independent small problems, each one optimizing \mathbf{u}_i , $\mathbf{u}_i = \arg \min_{\mathbf{x} \in \mathbb{R}^r} L(\mathbf{x} | \mathbf{V}^{(t)})$,

$$\begin{aligned} \mathbf{u}_i = \arg \min_{\mathbf{x} \in \mathbb{R}^r} \left\{ \|\mathbf{y}_i - \mathbf{V}^{(t)} \mathbf{x}\|_{\ell_1} + \lambda_1 \sum_{l=1}^r \min \left(\frac{|x_l|}{\tau_1}, 1 \right) \right. \\ \left. + \lambda_2 \sum_{l < l': (l, l') \in \mathcal{E}_{\mathbf{v}_j}} \min \left(\frac{|x_l - x_{l'}|}{\tau_2}, 1 \right) + \lambda_3 \sum_{l=1}^r x_l^2 \right\}, \end{aligned} \quad (4.3)$$

where λ_1 is a parameter controlling the sparsity and λ_2 controls the grouping effect. Problem (4.2) can be decomposed into n independent small subproblems, each optimizing with respect to \mathbf{v}_j , with similar structures. We propose an alternating minimization framework to solve the GRMF problem (Algorithm 1), by updating \mathbf{U} and \mathbf{V} alternatively until convergence.

Theorem 1 (Global Convergence of GRMF). *Let \mathbf{Y} be a matrix in $\mathbb{R}^{d \times n}$. Let $\{(\mathbf{U}^{(t)}, \mathbf{V}^{(t)})\}_{t \in \mathbb{N}}$ be a bounded sequence generated by Algorithm 1 to solve GRMF, with $\lambda_1, \lambda_2, \lambda_3, \tau_1, \tau_2$ appropriately selected. Then the sequence has finite length and converges to a critical point.*

As for convergence analysis, Theorem 1 gives a convergence guarantee of the alternative minimization framework to solve the GRMF problem. The main theorem of Csiszár and Tusnády (1984) (Theorem 3) proves a general convergence behavior of alternating minimization, and Hardt (2014) (Theorem 3.8) proves the convergence of a specific application of alternating minimization algorithm in MF. As a special case of alternating minimization applied in MF, the convergence behavior of GRMF is thus summarized in Theorem 1. The proof just mimics the proof of Theorem 3.8 in Hardt (2014), and we omit the details, as Algorithm 1 is a special case of alternating minimization algorithm applied in MF.

Limitation of the model One limitation of GRMF is that it uses non-convex regularizers which are neither smooth nor differentiable. Na et al. (2019) has pointed out that, when using non-convex penalties, iterative methods such as gradient or coordinate descent may terminate undesirably at a local optimum, which can be different from the global optimum we pursue. As is pointed out in Wen et al. (2018), the performance of non-convex optimization problems is usually closely related to the initialization. These are the inherent drawbacks of non-convex optimization problems.

4.2 General formulation for each GRMF subproblem

The minimization problem (4.3) can be viewed as a special form of the following constrained regression-type optimization problem with simultaneous supervised grouping and feature selection,

$$\min_{\mathbf{x} \in \mathbb{R}^r} \|\mathbf{A}\mathbf{x} - \mathbf{b}\|_{\ell_1} + \lambda_1 \sum_{l=1}^r \min\left(\frac{|x_l|}{\tau_1}, 1\right) + \lambda_2 \sum_{l < l': (l, l') \in \mathcal{E}} \min\left(\frac{|x_l - x_{l'}|}{\tau_2}, 1\right) + \lambda_3 \sum_{l=1}^r x_l^2. \quad (4.4)$$

The notation $\mathbf{b} \in \mathbb{R}^n$ in (4.4) corresponds to $\mathbf{y}_i \in \mathbb{R}^n$ in (4.3), and $\mathbf{A} \in \mathbb{R}^{n \times r}$ corresponds to $\mathbf{V}^{(t)} \in \mathbb{R}^{n \times r}$. Thus $\|\mathbf{A}\mathbf{x} - \mathbf{b}\|_{\ell_1} = \sum_{i=1}^n |b_i - \mathbf{a}_i^T \mathbf{x}|$, where $\mathbf{a}_i \in \mathbb{R}^r$. Here λ_1, λ_2 are positive tuning parameters controlling feature sparsity and grouping effect, $\lambda_3 > 0$ is to prevent overfitting, $\tau_1 > 0$ is a thresholding parameter determining when a large regression coefficient will be penalized in the model, and $\tau_2 > 0$ determines when a large difference between two coefficients will be penalized. $\mathcal{E} \subset \{1, \dots, r\}^2$ denotes a set of edges between distinct nodes $l \neq l'$ for a complete undirected graph, with $l \sim l'$ representing an edge directly connecting two nodes. Note that the edge information on the complete undirected graph \mathcal{E} is unknown, and need be learned from the model.

The DC algorithm To solve problem (4.4), considering the non-smooth property of the ℓ_1 loss, we use a smooth approximation $|b_i - \mathbf{a}_i^T \mathbf{x}| \approx ((b_i - \mathbf{a}_i^T \mathbf{x})^2 + \epsilon)^{1/2}$, where ϵ is chosen to be a very small positive value, e.g. 10^{-6} . For each alternative minimization, we need to solve the following optimization problem, Then optimization problem (4.4) becomes minimizing

$$S(\mathbf{x}) = \sum_{i=1}^n ((b_i - \mathbf{a}_i^T \mathbf{x})^2 + \epsilon)^{1/2} + \lambda_1 \sum_{l=1}^r \min\left(\frac{|x_l|}{\tau_1}, 1\right) + \lambda_2 \sum_{l < l': (l, l') \in \mathcal{E}} \min\left(\frac{|x_l - x_{l'}|}{\tau_2}, 1\right) + \lambda_3 \|\mathbf{x}\|_2^2.$$

By applying $\min(a, b) = a - (a - b)_+$, the two regularizers can be rewritten and $S(\mathbf{x})$ can be decomposed into a difference of two convex functions, $S_1(\mathbf{x}) - S_2(\mathbf{x})$, which are defined as follows respectively,

$$\begin{aligned} S_1(\mathbf{x}) &= \sum_{i=1}^n ((b_i - \mathbf{a}_i^T \mathbf{x})^2 + \epsilon)^{1/2} + \lambda_1 \sum_{l=1}^r \frac{|x_l|}{\tau_1} + \lambda_2 \sum_{l < l': (l, l') \in \mathcal{E}} \frac{|x_l - x_{l'}|}{\tau_2} + \lambda_3 \sum_{l=1}^r x_l^2 \\ S_2(\mathbf{x}) &= \lambda_1 \sum_{l=1}^r \left(\frac{|x_l|}{\tau_1} - 1\right)_+ + \lambda_2 \sum_{l < l': (l, l') \in \mathcal{E}} \left(\frac{|x_l - x_{l'}|}{\tau_2} - 1\right)_+. \end{aligned}$$

At the m -th iteration, $S_2(\mathbf{x})$ should be linearized as a linear approximation of $S_2(\mathbf{x})$ at $(m-1)$ -th iteration. Thus, for the m -th minimization, we need to solve the following subproblem (see [Appendix A.1](#) for details)

$$S^{(m)}(\mathbf{x}) = \sum_{i=1}^n ((b_i - \mathbf{a}_i^T \mathbf{x})^2 + \epsilon)^{1/2} + \frac{\lambda_1}{\tau_1} \sum_{l \in \mathcal{F}^{(m-1)}} |x_l| + \frac{\lambda_2}{\tau_2} \sum_{l < l': (l, l') \in \mathcal{E}^{(m-1)}} |x_l - x_{l'}| + \lambda_3 \|\mathbf{x}\|_2^2, \quad (4.5)$$

where

$$\begin{aligned} \mathcal{F}^{(m-1)} &= \left\{ l : |\hat{x}_l^{(m-1)}| < \tau_1 \right\}, \\ \mathcal{E}^{(m-1)} &= \left\{ (l, l') \in \mathcal{E}, |\hat{x}_l^{(m-1)} - \hat{x}_{l'}^{(m-1)}| < \tau_2 \right\}. \end{aligned} \quad (4.6)$$

Here $\hat{\mathbf{x}}^{(m)} = \arg \min_{\mathbf{x}} S^{(m)}(\mathbf{x})$, and $\hat{\mathbf{x}}^{(m-1)}$ is the result at the $(m-1)$ -th iteration. Denote $x_{ll'} = x_l - x_{l'}$, and define $\boldsymbol{\xi} = (x_1, \dots, x_r, x_{12}, \dots, x_{1r}, \dots, x_{(r-1)r})$. The m -th subproblem (4.5) can be reformulated as an equality-constrained convex optimization problem,

$$S^{(m)}(\boldsymbol{\xi}) = \sum_{i=1}^n ((b_i - \mathbf{a}_i^T \mathbf{x})^2 + \epsilon)^{1/2} + \frac{\lambda_1}{\tau_1} \sum_{l \in \mathcal{F}^{(m-1)}} |x_l| + \frac{\lambda_2}{\tau_2} \sum_{l < l': (l, l') \in \mathcal{E}^{(m-1)}} |x_{ll'}| + \lambda_3 \|\mathbf{x}\|_2^2, \quad (4.7)$$

subject to $x_{ll'} = x_l - x_{l'}$, $\forall l < l' : (l, l') \in \mathcal{E}^{(m-1)}$.

Alternating direction method of multipliers In this step, at each iteration, a quadratic problem with linear equality constraints is solved by the augmented Lagrange method. The augmented Lagrangian form of (4.7) is as follows (see details in [Appendix A.2](#))

$$L_\nu^{(m)}(\boldsymbol{\xi}, \boldsymbol{\tau}) = S^{(m)}(\boldsymbol{\xi}) + \sum_{l < l': (l, l') \in \mathcal{E}^{(m-1)}} \tau_{ll'} (x_l - x_{l'} - x_{ll'}) + \frac{\nu}{2} \sum_{l < l': (l, l') \in \mathcal{E}^{(m-1)}} (x_l - x_{l'} - x_{ll'})^2.$$

Here $\tau_{ll'}$ and ν are the Lagrangian multipliers for the linear constraints and for the computational acceleration. Update $\tau_{ll'}$ and ν , with a constant value $\alpha > 1$ to accelerate the convergence,

$$\tau_{ll'}^{k+1} = \tau_{ll'}^k + \nu^k (\hat{x}_l^{(m,k)} - \hat{x}_{l'}^{(m,k)} - \hat{x}_{ll'}^{(m,k)}), \quad \nu^{k+1} = \alpha \nu^k. \quad (4.8)$$

To compute $\hat{\boldsymbol{\xi}}^{(m,k)} = \arg \min_{\boldsymbol{\xi}} L_\nu^{(m)}(\boldsymbol{\xi}, \boldsymbol{\tau}^k)$, we use ADMM and alternatively update between \mathbf{x} and $x_{ll'}$, while fixing $\tau_{ll'}^k$ and ν^k (for $k = 1, 2, \dots$). The following two items give the final results (check the details in [Appendix A.3](#)).

- Given $\hat{x}_l^{(m,k-1)}$, update $\hat{x}_l^{(m,k)}$ by

$$\hat{x}_l^{(m,k)} = \alpha^{-1} \gamma \quad (l = 1, \dots, r), \quad (4.9)$$

where

$$\alpha = \sum_{i=1}^n D_i^{-\frac{1}{2}} A_{il}^2 + 2\lambda_3 + \nu^k \left| l' : (l, l') \in \mathcal{E}^{(m-1)} \right|.$$

Let

$$\gamma^* = \sum_{i=1}^n D_i^{-\frac{1}{2}} c_{il} - \sum_{l < l': (l, l') \in \mathcal{E}^{(m-1)}} \tau_{ll'}^k + \nu^k \sum_{l < l': (l, l') \in \mathcal{E}^{(m-1)}} (\hat{x}_{l'}^{(m,k-1)} + \hat{x}_{ll'}^{(m,k-1)}).$$

Then $\gamma = \gamma^*$ if $|\hat{x}_l^{(m-1)}| \geq \tau_1$; otherwise $\gamma = \text{ST}(\gamma^*, \frac{\lambda_1}{\tau_1})$. $\text{ST}(\cdot, a)$ is the soft threshold function $\text{ST}(b, a) = \text{sign}(b)(|b| - a)_+$. Here $D_i = (b_i - \mathbf{a}_i^T \hat{\mathbf{x}}^{(m,k-1)})^2 + \epsilon$, and $c_{il} = A_{il}(b_i - \mathbf{a}_{i,-l}^T \hat{\mathbf{x}}_{-l}^{(m,k-1)})$. $\mathbf{a}_{i,-l}$ is the i -th row vector of \mathbf{A} without the l -th column, and $\hat{\mathbf{x}}_{-l}^{(m,k-1)}$ is the same as $\hat{\mathbf{x}}^{(m,k-1)}$ without the l -th element. ϵ is often set to be a small positive constant 10^{-6} .

- Given $\hat{x}_{ll'}^{(m,k-1)}$, update $\hat{x}_{ll'}^{(m,k)}$ (with $\hat{x}_l^{(m,k)}$ already updated and fixed).

$$\hat{x}_{ll'}^{(m,k)} = \begin{cases} \frac{1}{\nu^k} \text{ST} \left(\tau_{ll'}^k + \nu^k (\hat{x}_l^{(m,k)} - \hat{x}_{l'}^{(m,k)}), \frac{\lambda_2}{\tau_2} \right), & \text{if } (l, l') \in \mathcal{E}^{(m-1)} \\ \hat{x}_{ll'}^{(m-1)}, & \text{if } (l, l') \notin \mathcal{E}^{(m-1)} \end{cases}. \quad (4.10)$$

5 Experiments

Now that we have presented our GRMF model in detail, we turn to its experimental validation by conducting experiments using real data sets and evaluate the performance of GRMF. The biggest concern of our algorithm is to achieve the grouping effect and sparsity simultaneously, while keeping the reconstruction error at a low level, and to demonstrate the robustness to outliers and corruption noise. We compare GRMF with several state-of-the-art matrix factorization methods, which include Truncated SVD ([Hansen, 1987](#)), RPCA ([Candès et al., 2011](#)), RNMF ([Wen et al., 2018](#)), RPMF ([Wang et al., 2012](#)) and GoDec+ ([Guo et al., 2017](#)). GRMF is our main method with ℓ_1 -loss, GMF-L2 is its variant with ℓ_2 -loss. We first study the behaviors of the 7 algorithms against different ranks and corruption ratios. We then apply all the algorithms to the face recovery problem. The desktop computer used to run our experiments has 2.7 GHz 64-bit Intel Core i5 processor (with two cores) and 8GB RAM.

Algorithm 2: The DC-ADMM algorithm for \mathbf{u}_i updating

Input: Initialization $\mathbf{x}^{(0)}$, tuning parameters $\lambda_1, \lambda_2, \lambda_3, \tau_1, \tau_2$.

Result: $\mathbf{u}_i^{(t)}$. The resulting \mathbf{x} is assigned to $\mathbf{u}_i^{(t)}$.

Assign $\mathcal{F}^{(0)}, \mathcal{E}^{(0)}$ given $\hat{\mathbf{x}}^{(0)}$. Assign $\hat{x}_{l'}^{(0)} = \hat{x}_l^{(0)} - \hat{x}_{l'}^{(0)}, \forall l < l' (l, l') \in \mathcal{E}^{(0)}, m=1$;

$\hat{\mathbf{x}}^{(m,0)} = \hat{\mathbf{x}}^{(m-1)}, \hat{x}_{l'}^{(m,0)} = \hat{x}_{l'}^{(m-1)} \quad \forall l < l' \text{ and } (l, l') \in \mathcal{E}^{(0)}$;

```
while  $\|\hat{x}_l^{(m)} - \hat{x}_l^{(m-1)}\|_2^2 > \epsilon_{\text{outer}}$  do
   $m \leftarrow m + 1$ ;
  Update  $\mathcal{F}^{(m)}, \mathcal{E}^{(m)}$  by (4.6) given  $\hat{\mathbf{x}}^{(m)}$ ;
   $\hat{x}_{l'}^{(m)} = \hat{x}_l^{(m)} - \hat{x}_{l'}^{(m)}, \forall l < l' \text{ and } (l, l') \in \mathcal{E}^{(m)}$ ;
  while  $\|\hat{x}_l^{(m,k)} - \hat{x}_l^{(m,k-1)}\|_2^2 > \epsilon_{\text{inner}}$  do
     $k \leftarrow k + 1$ ;
    Update  $\tau_{l'}^k$  and  $\nu^k$  by (4.8);
    Update  $\hat{x}_l^{(m,k)}$  by (4.9);
    Update  $\hat{x}_{l'}^{(m,k)}$  by (4.10);
  end
end
```

5.1 Performance under different corruption ratios and reduced ranks

The reduced rank and the corruption ratio can have a strong impact on the performance and the robustness of matrix factorization methods. Thus the performance caused by these two factors should be thoroughly investigated in comparison of different matrix factorization methods. In this section, we show the behaviors of the 7 algorithms against different ranks and corruption ratios with a pilot experiment of one randomly chosen image from the Yale B dataset.

Robustness vs. corruption ratio In order to explore the robustness of the algorithms with the corruption ratio, we track the trajectory of the reconstruction errors with varying corruption ratios, while fixing the reduced rank. The reduced rank of 4 is used to demonstrate the performance of different MF methods, as too large a value might cause overfitting. The relative mean absolute error (Relative MAE) is used as a measure of reconstruction error, which is calculated by comparing the original image with the approximated image using the formula $\frac{\|\mathbf{Y} - \mathbf{U}\mathbf{V}^T\|_{\ell_1}}{\|\mathbf{Y}\|_{\ell_1}}$. Since the Relative MAE uses the ℓ_1 -norm loss, it can be viewed as the criterion to measure the robustness of different MF methods. The type of corruption is salt and pepper noise, which is commonly used in computer vision applications. We add it to the original image by randomly masking part of the pixels in the image with the value of 0 or 255 under given corruption ratio. For example, a 50% corruption ratio means half of the pixels in a image is replaced by either 0 or 255 with equal probability.

Figure 1a shows that both GRMF and RPMF can maintain the robustness with the lowest reconstruction errors, even when the corruption ratio gets very large. Their errors increase slowly with the increase of the corruption ratio, and even when half of the pixels are corrupted with a corruption ratio of 50% their errors will only increase slightly. In particular, when the corruption ratio between the corrupted image and the original image is above 50%, GRMF and RPMF can still reduce the reconstruction error to around 0.2. It is also worth mentioning that RPCA can always recover the raw input images perfectly, but it does not have the ability to deal with the corrupted images with noise. This behavior results from the formulation of RPCA that it is not modeling the latent factors, and that it does not take rank as a parameter, which also explains that RPCA keeps almost all the information of the input image and its error increases linearly with the corruption ratio.

Robustness vs. reduced rank In order to explore the robustness of the algorithms with the reduced rank, we track the trajectory of the reconstruction errors with varying reduced ranks, while fixing the corruption ratio. The corruption ratio of 50% salt and pepper noise is used to demonstrate the performance of different MF methods, as most of the other MF methods fail to reconstruct the image except for GRMF and RPMF.

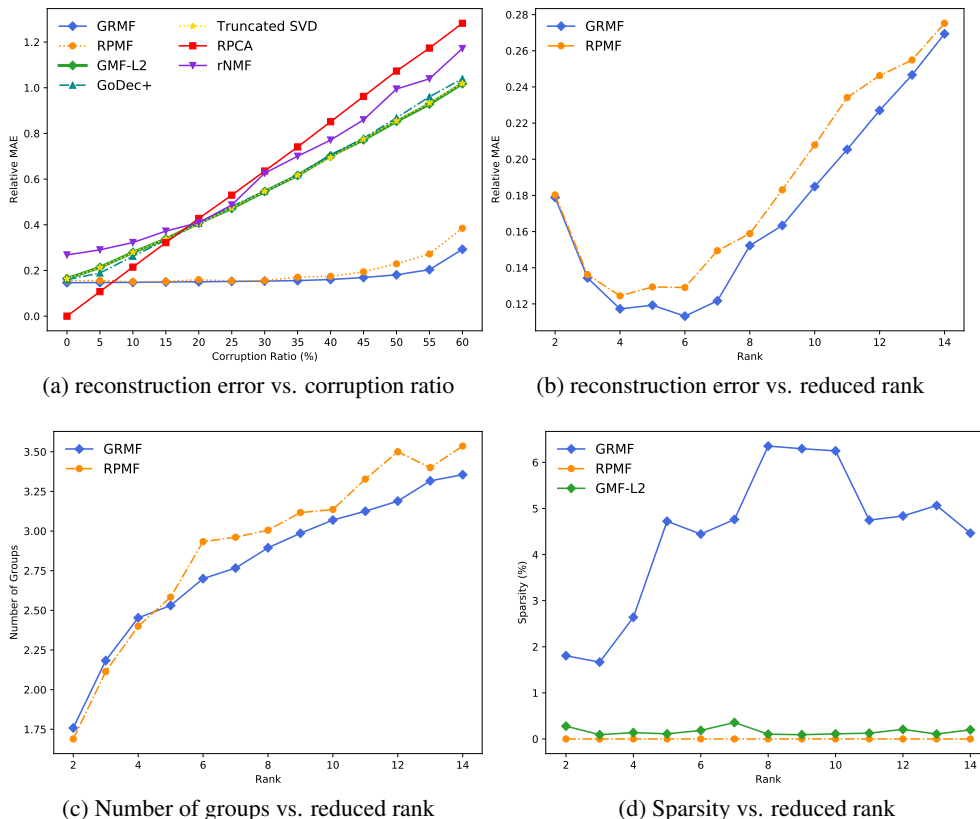


Figure 1: Performance under different corruption ratios and reduced ranks.

Table 1: Datasets information. We randomly choose some images of the same person/item, as the images for the same objective are very similar except in different angles/expressions/light conditions. The optimal rank for each dataset is reported on the fourth row. For the corrupted images, the rank is chosen to be one less than the optimal rank to avoid fitting the noise.

Datasets	Yale B	COIL20	ORL	JAFFE
Number of images	210	206	200	213
Size of images	192×168	128×128	112×92	180×150
Optimal rank	5	5	4	5

We run GRMF and RMPF with different ranks, since they are the only two algorithms that could well recover the original image under 50% corruption ratio. The results from Figure 1b show that the reconstruction error remains at a low level when the reduced ranks are relatively small, and it first decreases then starts to increase as the reduced rank gets larger and larger, which shows a potential of overfitting. Specifically, the reconstruction error of RMPF starts to increase when the reduced rank is bigger than 5, while the error of GRMF starts to increase when the reduced rank is bigger than 7, which shows that RMPF starts to overfit much earlier than GRMF. Obviously, the grouping effect of GRMF helps denoising the factorization and makes it less sensitive to the choice of the reduced rank. However, both GRMF and RMPF learn the noise and overfit the image as the rank gets too large. In addition, GRMF and RMPF have similar performance regarding the error, but GRMF has stronger grouping effect and sparsity, as illustrated in Figure 1c and Figure 1d. GRMF tends to have less number of groups and higher sparsity than RMPF.

5.2 Image recovery

Now we consider the application to image recovery in computer vision. We apply all the 7 algorithms on 4 datasets, Extended Yale B (Georghiades et al., 2001), COIL20 (Nene et al., 1996), ORL (Samaria et al., 1994), and JAFFE (Lyons et al., 1998). To avoid overfitting, we try several ranks and find an optimal rank in each situation. Table 1 reports the basic information about the datasets. We conduct the experiment on the original image and its 50% corrupted version. The results on Table 2 show that our GRMF algorithm has a better recovery ability than the other algorithms, especially under severe corruption. After running experiment over all the images in each dataset, we report the mean and the standard deviation of the relative MAE of the seven algorithms. All the algorithms perform well when there is no corruption, but only GRMF and PRMF remain at a low level with respect to the reconstruction error under 50% corruption. GRMF has the lowest reconstruction error under all cases while exhibiting a low standard deviation. On average, each image costs less than 300s. And the parallelizable nature of our algorithm allows a multiprocessing or multithreading settings to accelerate the computation. More results are reported on Appendix C.

Table 2: Comparison of the reconstruction errors on the 4 datasets. The average of the relative mean absolute error (RMAE) is reported with the standard deviation in the parentheses. For the corrupted images, we randomly masked 50% of the pixels in each image with salt and pepper noise. Note that we report RPCA only on the corrupted case. T-SVD stands for Truncated SVD.

Methods	Yale B		COIL		ORL		JAFFE	
	Origin	Corrupted	Origin	Corrupted	Origin	Corrupted	Origin	Corrupted
GRMF	0.093 ±(0.022)	0.143 ±(0.041)	0.123 ±(0.066)	0.245 ±(0.135)	0.105 ±(0.020)	0.204 ±(0.036)	0.121 ±(0.013)	0.165 ±(0.018)
PRMF	0.095±(0.023)	0.154±(0.047)	0.127±(0.070)	0.273±(0.142)	0.107±(0.020)	0.210±(0.037)	0.125±(0.014)	0.182±(0.025)
GMF-L2	0.103±(0.026)	0.555±(0.367)	0.143±(0.075)	0.821±(0.467)	0.114±(0.021)	0.320±(0.052)	0.133±(0.013)	0.398±(0.055)
GoDec+	0.101±(0.025)	0.565±(0.370)	0.139±(0.074)	0.830±(0.470)	0.113±(0.022)	0.325±(0.053)	0.132±(0.013)	0.412±(0.058)
T-SVD	0.103±(0.026)	0.560±(0.368)	0.143±(0.075)	0.824±(0.469)	0.114±(0.021)	0.324±(0.052)	0.133±(0.013)	0.401±(0.056)
RPCA	-	0.835±(0.380)	-	0.963±(0.446)	-	0.577±(0.073)	-	0.608±(0.078)
RNMF	0.149±(0.053)	0.626±(0.393)	0.285±(0.280)	0.722±(0.214)	0.130±(0.025)	0.360±(0.055)	0.207±(0.022)	0.456±(0.064)

6 Conclusion

In this work, we studied the problem of matrix factorization incorporating sparsity and grouping effect. We proposed a novel method, namely *Robust Matrix Factorization with Grouping effect* (GRMF), which intends to lower the reconstruction errors while promoting interpretability of the solution through automatically determining the number of latent groups in the solution. To the best of our knowledge, it is the first paper to introduce the automatic learning of grouping effect without prior information into MF. Specifically, GRMF incorporates two novel non-convex regularizers that control both sparsity and grouping effect in the objective function, and a novel optimization framework is proposed to obtain the solution. Moreover, GRMF employs an alternative minimization procedure to decompose the problem into a number of coupled non-convex subproblems, where each subproblem optimizes a row or a column in the solution of MF through difference-of-convex (DC) programming and the alternating direction method of multipliers (ADMM). We have conducted extensive experiments to evaluate GRMF using (1) Extended Yale B dataset under different rank choices and corruption ratios and (2) image reconstruction tasks on 4 image datasets (COIL-20, ORL, Extended Yale B, and JAFFE) under 50% corruption ratio. Compared with 6 baseline algorithms, GRMF has achieved the best reconstruction accuracy in both tasks, while demonstrating the performance advances from the use of grouping effects and sparsity, especially under severe data corruption.

References

- Maryam Abdolali and Nicolas Gillis. Simplex-structured matrix factorization: Sparsity-based identifiability and provably correct algorithms. *SIAM Journal on Mathematics of Data Science*, 3(2):593–623, 2021.
- Emmanuel J Candès, Xiaodong Li, Yi Ma, and John Wright. Robust principal component analysis? *Journal of the ACM (JACM)*, 58(3):1–37, 2011.
- Yuejie Chi, Yue M Lu, and Yuxin Chen. Nonconvex optimization meets low-rank matrix factorization: An overview. *IEEE Transactions on Signal Processing*, 67(20):5239–5269, 2019.

- Seungjin Choi. Algorithms for orthogonal nonnegative matrix factorization. In *2008 IEEE International Joint Conference on Neural Networks (IEEE World Congress on Computational Intelligence)*, pages 1828–1832. IEEE, 2008.
- I. Csizsár and G. Tusnády. Information geometry and alternating minimization procedures. *Statistics & Decisions*, (1):205–237, 1984.
- Zhen Cui, Jin-Xing Liu, Ying-Lian Gao, Chun-Hou Zheng, and Juan Wang. Rcmf: a robust collaborative matrix factorization method to predict mirna-disease associations. *BMC bioinformatics*, 20(25):1–10, 2019.
- Xiangguang Dai, Xiaojie Su, Wei Zhang, Fangzheng Xue, and Huaqing Li. Robust manhattan non-negative matrix factorization for image recovery and representation. *Information Sciences*, 527:70–87, 2020.
- Hongbo Gao, Fang Guo, Juping Zhu, Zhen Kan, and Xinyu Zhang. Human motion segmentation based on structure constraint matrix factorization. *Inform. Sci.*, 2022(65):119103, 2022.
- Renaud Gaujoux and Cathal Seoighe. A flexible R package for nonnegative matrix factorization. *BMC bioinformatics*, 11(1):1–9, 2010.
- A.S. Georghiades, P.N. Belhumeur, and D.J. Kriegman. From few to many: Illumination cone models for face recognition under variable lighting and pose. *IEEE Trans. Pattern Anal. Mach. Intelligence*, 23(6):643–660, 2001.
- Kailing Guo, Liu Liu, Xiangmin Xu, Dong Xu, and Dacheng Tao. Godec+: Fast and robust low-rank matrix decomposition based on maximum correntropy. *IEEE transactions on neural networks and learning systems*, 29(6):2323–2336, 2017.
- Davide Feltoni Gurini, Fabio Gasparetti, Alessandro Micarelli, and Giuseppe Sansonetti. Temporal people-to-people recommendation on social networks with sentiment-based matrix factorization. *Future Generation Computer Systems*, 78:430–439, 2018.
- Benjamin Haeffele, Eric Young, and Rene Vidal. Structured low-rank matrix factorization: Optimality, algorithm, and applications to image processing. In *International conference on machine learning*, pages 2007–2015. PMLR, 2014.
- Benjamin D Haeffele and René Vidal. Structured low-rank matrix factorization: Global optimality, algorithms, and applications. *IEEE transactions on pattern analysis and machine intelligence*, 42(6):1468–1482, 2019.
- Per Christian Hansen. The truncatedsvd as a method for regularization. *BIT Numerical Mathematics*, 27(4):534–553, 1987.
- Moritz Hardt. Understanding alternating minimization for matrix completion. In *2014 IEEE 55th Annual Symposium on Foundations of Computer Science*, pages 651–660. IEEE, 2014.
- Patrik O Hoyer. Non-negative matrix factorization with sparseness constraints. *Journal of machine learning research*, 5(9), 2004.
- Martin Jakomin, Zoran Bosnić, and Tomaž Curk. Simultaneous incremental matrix factorization for streaming recommender systems. *Expert Systems with Applications*, 160:113685, 2020.
- Ali Akbar Jamali, Anthony Kusalik, and Fang-Xiang Wu. Mdipa: a microRNA–drug interaction prediction approach based on non-negative matrix factorization. *Bioinformatics*, 36(20):5061–5067, 2020.
- Jingu Kim, Renato DC Monteiro, and Haesun Park. Group sparsity in nonnegative matrix factorization. In *Proceedings of the 2012 SIAM International Conference on Data Mining*, pages 851–862. SIAM, 2012.
- Virginia Klema and Alan Laub. The singular value decomposition: Its computation and some applications. *IEEE Transactions on automatic control*, 25(2):164–176, 1980.

- Yehuda Koren, Robert Bell, and Chris Volinsky. Matrix factorization techniques for recommender systems. *Computer*, 42(8):30–37, 2009.
- Fangfang Li, Guandong Xu, Longbing Cao, Xiaozhong Fan, and Zhendong Niu. Cgmf: Coupled group-based matrix factorization for recommender system. In *International Conference on Web Information Systems Engineering*, pages 189–198. Springer, 2013.
- Ruyue Li, Lefei Zhang, and Bo Du. A robust dimensionality reduction and matrix factorization framework for data clustering. *Pattern Recognition Letters*, 128:440–446, 2019.
- Zhouchen Lin, Chen Xu, and Hongbin Zha. Robust matrix factorization by majorization minimization. *IEEE transactions on pattern analysis and machine intelligence*, 40(1):208–220, 2017.
- Michael Lyons, Miyuki Kamachi, and Jiro Gyoba. The Japanese Female Facial Expression (JAFFE) Dataset, April 1998. URL <https://doi.org/10.5281/zenodo.3451524>. The images are provided at no cost for non-commercial scientific research only. If you agree to the conditions listed below, you may request access to download.
- Hao Ma, Haixuan Yang, Michael R Lyu, and Irwin King. Sorec: social recommendation using probabilistic matrix factorization. In *Proceedings of the 17th ACM conference on Information and knowledge management*, pages 931–940, 2008.
- Andriy Mnih and Russ R Salakhutdinov. Probabilistic matrix factorization. *Advances in neural information processing systems*, 20:1257–1264, 2007.
- Hanwool Na, Myeongmin Kang, Miyoung Jung, and Myungjoo Kang. Nonconvex tgv regularization model for multiplicative noise removal with spatially varying parameters. *Inverse Problems & Imaging*, 13(1):117, 2019.
- Sameer A. Nene, Shree K. Nayar, and Hiroshi Murase. Columbia object image library (coil-20). Technical report, 1996.
- Fernando Ortega, Antonio Hernando, Jesus Bobadilla, and Jeon Hyung Kang. Recommending items to group of users using matrix factorization based collaborative filtering. *Information Sciences*, 345:313–324, 2016.
- Hashem Parvin, Parham Moradi, Shahrokh Esmaeili, and Nooruldeen Nasih Qader. A scalable and robust trust-based nonnegative matrix factorization recommender using the alternating direction method. *Knowledge-Based Systems*, 166:92–107, 2019.
- Alberto Pascual-Montano, Pedro Carmona-Saez, Monica Chagoyen, Francisco Tirado, Jose M Carazo, and Roberto D Pascual-Marqui. bionmf: a versatile tool for non-negative matrix factorization in biology. *BMC bioinformatics*, 7(1):1–9, 2006.
- Alireza Rahimpour, Hairong Qi, David Fugate, and Teja Kuruganti. Non-intrusive energy disaggregation using non-negative matrix factorization with sum-to-k constraint. *IEEE Transactions on Power Systems*, 32(6):4430–4441, 2017.
- F. S. Samaria, F. S. Samaria *t, A.C. Harter, and Old Addenbrooke’s Site. Parameterisation of a stochastic model for human face identification, 1994.
- Xiaotong Shen, Wei Pan, and Yunzhang Zhu. Likelihood-based selection and sharp parameter estimation. *Journal of the American Statistical Association*, 107(497):223–232, 2012.
- Nathan Srebro, Jason Rennie, and Tommi S Jaakkola. Maximum-margin matrix factorization. In *Advances in neural information processing systems*, pages 1329–1336, 2005.
- Naiyan Wang and Dit-Yan Yeung. Bayesian robust matrix factorization for image and video processing. In *Proceedings of the IEEE International Conference on Computer Vision*, pages 1785–1792, 2013.
- Naiyan Wang, Tiansheng Yao, Jingdong Wang, and Dit-Yan Yeung. A probabilistic approach to robust matrix factorization. In *European Conference on Computer Vision*, pages 126–139. Springer, 2012.

- Qi Wang, Xiang He, Xu Jiang, and Xuelong Li. Robust bi-stochastic graph regularized matrix factorization for data clustering. *IEEE Transactions on Pattern Analysis and Machine Intelligence*, 2020.
- Fei Wen, Lei Chu, Peilin Liu, and Robert C Qiu. A survey on nonconvex regularization-based sparse and low-rank recovery in signal processing, statistics, and machine learning. *IEEE Access*, 6: 69883–69906, 2018.
- Svante Wold, Kim Esbensen, and Paul Geladi. Principal component analysis. *Chemometrics and intelligent laboratory systems*, 2(1-3):37–52, 1987.
- Shuang Xu, Chunxia Zhang, and Jianshe Zhang. Bayesian deep matrix factorization network for multiple images denoising. *Neural Networks*, 123:420–428, 2020.
- Hong-Jian Xue, Xinyu Dai, Jianbing Zhang, Shujian Huang, and Jiajun Chen. Deep matrix factorization models for recommender systems. In *IJCAI*, volume 17, pages 3203–3209. Melbourne, Australia, 2017.
- Sen Yang, Lei Yuan, Ying-Cheng Lai, Xiaotong Shen, Peter Wonka, and Jieping Ye. Feature grouping and selection over an undirected graph. In *Proceedings of the 18th ACM SIGKDD international conference on Knowledge discovery and data mining*, pages 922–930, 2012.
- Quanming Yao and James Kwok. Scalable robust matrix factorization with nonconvex loss. *arXiv preprint arXiv:1710.07205*, 31, 2018. URL <https://proceedings.neurips.cc/paper/2018/file/2c3ddf4bf13852db711dd1901fb517fa-Paper.pdf>.
- Man-Ching Yuen, Irwin King, and Kwong-Sak Leung. Taskrec: probabilistic matrix factorization in task recommendation in crowdsourcing systems. In *International Conference on Neural Information Processing*, pages 516–525. Springer, 2012.
- Lijun Zhang, Zhengguang Chen, Miao Zheng, and Xiaofei He. Robust non-negative matrix factorization. *Frontiers of Electrical and Electronic Engineering in China*, 6(2):192–200, 2011.
- Yupei Zhang, Yue Yun, Huan Dai, Jiaqi Cui, and Xuequn Shang. Graphs regularized robust matrix factorization and its application on student grade prediction. *Applied Sciences*, 10(5):1755, 2020.

Appendices

Illustration of the grouping effect of GRMF

$$\begin{pmatrix} 100 & 110 & 90 & \dots & 200 & 190 & 210 \\ 100 & 110 & 90 & \dots & 200 & 190 & 210 \\ \vdots & \vdots & \vdots & & \vdots & \vdots & \vdots \\ 0.01 & 100 & 120 & \dots & 2.5 & 0.21 & 90 \end{pmatrix} \xrightarrow{\text{Grouping}} \begin{pmatrix} 101 & 99.5 & 100 & \dots & 200 & 199.5 & 201 \\ 100 & 100.5 & 99.5 & \dots & 201 & 200 & 199 \\ \vdots & \vdots & \vdots & & \vdots & \vdots & \vdots \\ 0.01 & 100 & 105 & \dots & 0.91 & 0.01 & 97.5 \end{pmatrix}$$

Figure 2: Illustration of grouping effect

We take the grouping effect in a matrix as an example. As shown in Figure 2, the grouping effect along each row of the matrix can introduce clustering between similar items, where elements close to each other are clustered in the same group which is highlighted with the same color. In addition, the elements clustered in the same group do not need to be adjacent. In the decomposed matrix obtained from GRMF, this grouping effect along the hidden factors is expected in both \mathbf{U} and \mathbf{V} .

A Details of the algorithm of GRMF

A Python implementation of GRMF can be found on [github](https://github.com/GroupingEffects/GRMF)².

A.1 Difference-of-convex algorithm (DC)

Note that the optimization problem of $L(\mathbf{U}|\mathbf{V})$ in (4.1) can be decomposed into d independent subproblems. The same procedure applies to the minimization of $L(\mathbf{V}|\mathbf{U})$ in (4.2). Thus, the problem of GRMF is a combination of $n + d$ optimization subproblems, each with respect to a vector in \mathbb{R}^r . For each alternative minimization, we need to solve the following optimization problem:

$$\arg \min_{\mathbf{x}} \left\{ S(\mathbf{x}) = \sum_{i=1}^n [(b_i - \mathbf{a}_i^T \mathbf{x})^2 + \epsilon]^{\frac{1}{2}} + \lambda_1 \sum_{l=1}^r \min \left(\frac{|x_l|}{\tau_1}, 1 \right) + \lambda_2 \sum_{l < l': (l, l') \in \mathcal{E}} \min \left(\frac{|x_l - x_{l'}|}{\tau_2}, 1 \right) + \lambda_3 \sum_{l=1}^r x_l^2 \right\}.$$

By applying that $\min(a, b) = a - (a - b)_+$, $S(\mathbf{x})$ can be decomposed into a difference of two convex functions as follows,

$$\begin{aligned} S_1(\mathbf{x}) &= \sum_{i=1}^n [(b_i - \mathbf{a}_i^T \mathbf{x})^2 + \epsilon]^{\frac{1}{2}} + \lambda_1 \sum_{l=1}^r \frac{|x_l|}{\tau_1} + \lambda_2 \sum_{l < l': (l, l') \in \mathcal{E}} \frac{|x_l - x_{l'}|}{\tau_2} + \lambda_3 \sum_{l=1}^r x_l^2, \\ S_2(\mathbf{x}) &= \lambda_1 \sum_{l=1}^r \left(\frac{|x_l|}{\tau_1} - 1 \right)_+ + \lambda_2 \sum_{l < l': (l, l') \in \mathcal{E}} \left(\frac{|x_l - x_{l'}|}{\tau_2} - 1 \right)_+. \end{aligned}$$

Approximation of the trailing convex function We then construct a sequence of approximations of $S_2(\mathbf{x})$ iteratively. At the m -th iteration, we approximate $S_2(\mathbf{x})$ by its affine minorization, by linearizing the trailing convex function $S_2(\mathbf{x})$.

By linearizing the trailing convex function $S_2(\mathbf{x})$ in the difference convex decomposition, we replace $S_2(\mathbf{x})$ at the m -th iteration with its affine minorization at $(m - 1)$ -th iteration. We linearize the

²<https://github.com/GroupingEffects/GRMF>

trailing convex function $S_2(\boldsymbol{\eta}) = S_2(\boldsymbol{\eta}^*) + \langle \boldsymbol{\eta} - \boldsymbol{\eta}^*, \partial S_2(\boldsymbol{\eta}^*) \rangle$ at a neighborhood of $\boldsymbol{\eta}^* \in \mathbb{R}^{(r^2+r)/2}$, where $\partial S_2(\boldsymbol{\eta})$ is the first derivative of $S_2(\boldsymbol{\eta})$ with respect to $\boldsymbol{\eta}$, and $\langle \cdot, \cdot \rangle$ is the inner product, where

$$\boldsymbol{\eta} = (|x_1|, |x_2|, \dots, |x_r|, |x_{12}|, \dots, |x_{1r}|, \dots, |x_{(r-1)r}|)^T.$$

Then we get

$$S(\boldsymbol{\eta}) = S(\boldsymbol{\eta}^*) + \langle \boldsymbol{\eta} - \boldsymbol{\eta}^*, \nabla S(\boldsymbol{\eta})|_{\boldsymbol{\eta}=\boldsymbol{\eta}^*} \rangle.$$

Thus, at the m -th iteration, we replace $S_2(\mathbf{x})$ with the m -th approximation by

$$S_2^{(m)}(\mathbf{x}) = \tilde{S}_2^{(m)}(\boldsymbol{\eta}) = \tilde{S}_2(\hat{\boldsymbol{\eta}}^{(m-1)}) + \langle \boldsymbol{\eta} - \hat{\boldsymbol{\eta}}^{(m-1)}, \partial \tilde{S}_2(\hat{\boldsymbol{\eta}}^{(m-1)}) \rangle.$$

Specifically,

$$\begin{aligned} S_2^{(m)}(\mathbf{x}) &= S_2(\hat{\mathbf{x}}^{(m-1)}) + \langle \mathbf{x} - \hat{\mathbf{x}}^{(m-1)}, \partial S_2(\mathbf{x})|_{\mathbf{x}=\hat{\mathbf{x}}^{(m-1)}} \rangle \\ &= S_2(\hat{\mathbf{x}}^{(m-1)}) + \frac{\lambda_1}{\tau_1} \sum_{l=1}^r I_{\{|\hat{x}_l^{(m-1)}| \geq \tau_1\}} \cdot (|x_l| - |\hat{x}_l^{(m-1)}|) \\ &\quad + \frac{\lambda_2}{\tau_2} \sum_{l < l': (l, l') \in \mathcal{E}} I_{\{|\hat{x}_l^{(m-1)} - \hat{x}_{l'}^{(m-1)}| \geq \tau_2\}} \cdot (|x_l - x_{l'}| - |\hat{x}_l^{(m-1)} - \hat{x}_{l'}^{(m-1)}|). \end{aligned} \quad (\text{A.1})$$

Finally, a sequence of approximations of $S(\mathbf{x})$ is constructed iteratively. For the m -th approximation, an upper convex approximating function to $S(\mathbf{x})$ can be obtained by $S^{(m)}(\mathbf{x}) = S_1(\mathbf{x}) - S_2^{(m)}(\mathbf{x})$, which formulates the following subproblem.

$$\min_{\mathbf{x}} \sum_{i=1}^n [(b_i - \mathbf{a}_i^T \mathbf{x})^2 + \epsilon]^{\frac{1}{2}} + \frac{\lambda_1}{\tau_1} \sum_{l \in \mathcal{F}^{(m-1)}} |x_l| + \frac{\lambda_2}{\tau_2} \sum_{l < l': (l, l') \in \mathcal{E}^{(m-1)}} |x_l - x_{l'}| + \lambda_3 \sum_{l=1}^r x_l^2. \quad (\text{A.2})$$

where

$$\begin{aligned} \mathcal{F}^{(m-1)} &= \{l : |\hat{x}_l^{(m-1)}| < \tau_1\}, \\ \mathcal{E}^{(m-1)} &= \{(l, l') \in \mathcal{E}, |\hat{x}_l^{(m-1)} - \hat{x}_{l'}^{(m-1)}| < \tau_2\}. \end{aligned} \quad (\text{A.3})$$

Denote $x_{ll'} = x_l - x_{l'}$ and define $\boldsymbol{\xi} = (x_1, \dots, x_r, x_{12}, \dots, x_{1r}, \dots, x_{(r-1)r})$. The m -th subproblem Eq.(A.2) can be reformulated as an equality-constrained convex optimization problem,

$$\min_{\boldsymbol{\xi}} \sum_{i=1}^n [(b_i - \mathbf{a}_i^T \mathbf{x})^2 + \epsilon]^{\frac{1}{2}} + \frac{\lambda_1}{\tau_1} \sum_{l \in \mathcal{F}^{(m-1)}} |x_l| + \frac{\lambda_2}{\tau_2} \sum_{l < l': (l, l') \in \mathcal{E}^{(m-1)}} |x_{ll'}| + \lambda_3 \sum_{l=1}^r x_l^2, \quad (\text{A.4})$$

subject to

$$x_{ll'} = x_l - x_{l'}, \forall l < l' : (l, l') \in \mathcal{E}^{(m-1)}.$$

For the equality-constrained problem Eq.(A.4), we employ the augmented Lagrange method to solve its equivalent unconstrained version iteratively with respect to k for the m -th approximation.

A.2 Alternating direction method of multipliers (ADMM)

To apply ADMM in our constrained optimization problem Eq.(A.4), we separate Eq.(A.4) in two parts:

$$\begin{aligned} f(\mathbf{x}) &= \sum_{i=1}^n [(b_i - \mathbf{a}_i^T \mathbf{x})^2 + \epsilon]^{\frac{1}{2}} + \frac{\lambda_1}{\tau_1} \sum_{l \in \mathcal{F}^{(m-1)}} |x_l| + \lambda_3 \sum_{l=1}^r x_l^2, \\ g(\mathbf{x}_{ll'}) &= \frac{\lambda_2}{\tau_2} \sum_{l < l': (l, l') \in \mathcal{E}^{(m-1)}} |x_{ll'}|, \end{aligned} \quad (\text{A.5})$$

subject to

$$x_l - x_{l'} = x_{ll'}, \quad \forall l < l', (l, l') \in \mathcal{E}^{(m-1)}.$$

With definition $\xi = (\mathbf{x}, \mathbf{x}_{ll'})$, the augmented Lagrangian for Eq.(A.5) is

$$L_\nu^{(m)}(\xi, \tau) = L_\nu^{(m)}(\mathbf{x}, \mathbf{x}_{ll'}, \tau) = f(\mathbf{x}) + g(\mathbf{x}_{ll'}) + \sum_{l < l': (l, l') \in \mathcal{E}^{(m-1)}} \tau_{ll'}(x_l - x_{l'} - x_{ll'}) + \frac{\nu}{2} \sum_{l < l': (l, l') \in \mathcal{E}^{(m-1)}} (x_l - x_{l'} - x_{ll'})^2, \quad (\text{A.6})$$

where $\tau_{ll'}$ and ν are the Lagrangian multipliers for the linear constraints and for the computational acceleration.

Minimizing Eq.(A.6) over $\xi = (\mathbf{x}, \mathbf{x}_{ll'})$ yields $\hat{\xi}^{(m,k)} = (\hat{\mathbf{x}}^{(m,k)}, \hat{\mathbf{x}}_{ll'}^{(m,k)})$ for given values of $(\tau_{ll'}^k, \nu^k)$. Note that as the iteration proceeds, $x_l - x_{l'}$ and $x_{ll'}$ becomes closer and closer, so we need ν to increase through the process. In particular, the ADMM updating rules are as follows

$$\mathbf{x}\text{-updating} \quad \hat{\mathbf{x}}^{(m,k+1)} = \arg \min_{\mathbf{x}} L_\nu^{(m)}(\mathbf{x}, \hat{\mathbf{x}}_{ll'}^{(m,k)}, \tau^k), \quad (\text{A.7})$$

$$\mathbf{x}_{ll'}\text{-updating} \quad \hat{\mathbf{x}}_{ll'}^{(m,k+1)} = \arg \min_{\mathbf{x}_{ll'}} L_\nu^{(m)}(\hat{\mathbf{x}}^{(m,k+1)}, \mathbf{x}_{ll'}, \tau^k), \quad (\text{A.8})$$

$$\tau_{ll'}\text{-updating} \quad \tau_{ll'}^{k+1} = \tau_{ll'}^k + \nu^k \left(\hat{x}_l^{(m,k+1)} - \hat{x}_{l'}^{(m,k+1)} - \hat{x}_{ll'}^{(m,k+1)} \right), \quad \nu^{k+1} = \rho \nu^k. \quad (\text{A.9})$$

Here ρ is some constant chosen larger than 1, which controls the acceleration of the algorithm. The details of the $\hat{\xi}^{(m,k)}$ minimization step can be found in the following two subsections.

A.3 The \mathbf{x} -updating

Updating $\hat{x}_l^{(m,k)}$ in ADMM We first write the function of \mathbf{x} as $H(\mathbf{x})$.

$$\begin{aligned} H(\mathbf{x}) &\triangleq L_\nu^{(m)}(\mathbf{x}, \hat{\mathbf{x}}_{ll'}^{(m,k)}, \tau^k) \\ &= \underbrace{\sum_{i=1}^n [(b_i - \mathbf{a}_i^T \mathbf{x})^2 + \epsilon]^{\frac{1}{2}}}_{\langle 1 \rangle} + \underbrace{\frac{\lambda_1}{\tau_1} \sum_{l \in \mathcal{F}^{(m-1)}} |x_l|}_{\langle 2 \rangle} + \underbrace{\lambda_3 \sum_{l=1}^r x_l^2}_{\langle 3 \rangle} \\ &+ \underbrace{\sum_{l < l': (l, l') \in \mathcal{E}^{(m-1)}} \tau_{ll'}^k (x_l - \hat{x}_{l'}^{(m,k-1)} - \hat{x}_{ll'}^{(m,k-1)})}_{\langle 4-1 \rangle} + \underbrace{\sum_{l > l': (l, l') \in \mathcal{E}^{(m-1)}} \tau_{ll'}^k (x_l - \hat{x}_{l'}^{(m,k)} - \hat{x}_{ll'}^{(m,k-1)})}_{\langle 4-2 \rangle} \\ &+ \underbrace{\frac{\nu^k}{2} \sum_{l < l': (l, l') \in \mathcal{E}^{(m-1)}} (x_l - \hat{x}_{l'}^{(m,k-1)} - \hat{x}_{ll'}^{(m,k-1)})^2}_{\langle 5-1 \rangle} + \underbrace{\frac{\nu^k}{2} \sum_{l > l': (l, l') \in \mathcal{E}^{(m-1)}} (x_l - \hat{x}_{l'}^{(m,k)} - \hat{x}_{ll'}^{(m,k-1)})^2}_{\langle 5-2 \rangle} \end{aligned}$$

We calculate the derivative of $H(\mathbf{x})$ part by part. Set the derivatives of $\langle 1 \rangle + \langle 2 \rangle + \langle 3 \rangle + \langle 4-1 \rangle + \langle 4-2 \rangle + \langle 5-1 \rangle + \langle 5-2 \rangle = 0$, we get an equation about x_l .

The x_l terms:

$$\sum_{i=1}^n D_i^{-\frac{1}{2}} A_{il}^2 x_l + 2\lambda_3 \cdot x_l + \nu^k \sum_{l < l': (l, l') \in \mathcal{E}^{(m-1)}} 1 \cdot x_l + \nu^k \sum_{l > l': (l, l') \in \mathcal{E}^{(m-1)}} 1 \cdot x_l$$

where

$$\nu^k \sum_{l < l': (l, l') \in \mathcal{E}^{(m-1)}} 1 \cdot x_l + \nu^k \sum_{l > l': (l, l') \in \mathcal{E}^{(m-1)}} 1 \cdot x_l = \nu^k \cdot \left| l' : (l, l') \in \mathcal{E}^{(m-1)} \right| \cdot x_l$$

and $\left| l' : (l, l') \in \mathcal{E}^{(m-1)} \right|$ is the number of the elements in the set.

The constant terms:

$$\begin{aligned}
& - \sum_{i=1}^n D_i^{-\frac{1}{2}} (b_i A_{il} - (\mathbf{a}_{i,-l} \widehat{\mathbf{x}}_{-l}^{(m,k-1)}) \cdot A_{il}) + \begin{cases} \frac{\lambda_1}{\tau_1} & \text{if } |\hat{x}_l^{(m-1)}| < \tau_1 \text{ and } x_l > 0 \\ -\frac{\lambda_1}{\tau_1} & \text{if } |\hat{x}_l^{(m-1)}| < \tau_1 \text{ and } x_l < 0 \\ 0 & \text{otherwise} \end{cases} \\
& + \sum_{(l,l') \in \mathcal{E}^{(m-1)}} \tau_{ll'}^k - \nu^k \sum_{(l,l') \in \mathcal{E}^{(m-1)}} (\hat{x}_{l'}^{(m,k-1)} + \hat{x}_{ll'}^{(m,k-1)})
\end{aligned}$$

Thus the updating of $\hat{x}_l^{(m,k)}$,

$$\hat{x}_l^{(m,k)} = \alpha^{-1} \gamma,$$

where

$$\alpha = \sum_{i=1}^n D_i^{-\frac{1}{2}} A_{il}^2 + 2\lambda_3 + \nu^k \left| l' : (l, l') \in \mathcal{E}^{(m-1)} \right|,$$

and

$$\gamma = \begin{cases} \gamma^*, & \text{if } |\hat{x}_l^{(m-1)}| \geq \tau_1 \\ \text{ST}(\gamma^*, \frac{\lambda_1}{\tau_1}), & \text{if } |\hat{x}_l^{(m-1)}| < \tau_1 \end{cases}.$$

ST is the soft threshold function,

$$\text{ST}(x, \delta) = \text{sign}(x)(|x| - \delta)_+ = \begin{cases} x - \delta, & \text{if } b > \delta \\ x + \delta, & \text{if } b < -\delta \\ 0, & \text{if } |b| \leq \delta \end{cases},$$

and

$$\gamma^* = \sum_{i=1}^n D_i^{-\frac{1}{2}} c_{il} - \sum_{l < l' : (l, l') \in \mathcal{E}^{(m-1)}} \tau_{ll'}^k + \nu^k \sum_{l < l' : (l, l') \in \mathcal{E}^{(m-1)}} (\hat{x}_{l'}^{(m,k-1)} + \hat{x}_{ll'}^{(m,k-1)}),$$

where $D_i = (b_i - \mathbf{a}_i^T \widehat{\mathbf{x}}^{(m,k-1)})^2 + \epsilon$, $c_{il} = A_{il} \cdot (b_i - \mathbf{a}_{i,-l}^T \widehat{\mathbf{x}}_{-l}^{(m,k-1)})$, $\mathbf{a}_{i,-l}$ is the i -th row vector of \mathbf{A} without the l -th column, and $\widehat{\mathbf{x}}_{(-l)}^{(m,k-1)}$ is the vector $\widehat{\mathbf{x}}^{(m,k-1)}$ without the l -th component.

A.4 The $\mathbf{x}_{ll'}$ -updating

Updating $\hat{x}_{ll'}^{(m,k)}$ in ADMM Given $\hat{x}_{ll'}^{(m,k-1)}$, update $\hat{x}_{ll'}^{(m,k)}$ ($1 \leq l < l' \leq r$) with $\hat{x}_l^{(m,k)}$ already updated and fixed.

$$\begin{aligned}
Q(\mathbf{x}_{ll'}) & \triangleq L_\nu^{(m)}(\widehat{\mathbf{x}}^{(m,k)}, \mathbf{x}_{ll'}, \boldsymbol{\tau}^k) \\
& = \underbrace{\frac{\lambda_2}{\tau_2} \sum_{l < l' : (l, l') \in \mathcal{E}^{(m-1)}} |x_{ll'}| + \tau_{ll'}^k}_{(I)} \underbrace{\sum_{l < l' : (l, l') \in \mathcal{E}^{(m-1)}} (\hat{x}_l^{(m,k)} - \hat{x}_{l'}^{(m,k)} - x_{ll'})}_{(II)} \\
& + \underbrace{\sum_{l < l' : (l, l') \in \mathcal{E}^{(m-1)}} \frac{\nu^k}{2} (\hat{x}_l^{(m,k)} - \hat{x}_{l'}^{(m,k)} - x_{ll'})^2}_{(III)}.
\end{aligned}$$

We calculate $\frac{\partial Q(\mathbf{x}_{ll'})}{\partial x_{ll'}}$ by part. Setting the derivative equals to zero, we have that

$$0 = \nu^k x_{ll'} - \tau_{ll'}^k - \nu^k (\hat{x}_l^{(m,k)} - \hat{x}_{l'}^{(m,k)}) + \begin{cases} \frac{\lambda_2}{\tau_2}, & \text{if } x_{ll'} > 0 \\ -\frac{\lambda_2}{\tau_2}, & \text{if } x_{ll'} < 0 \end{cases}.$$

Then

$$\hat{x}_{ll'}^{(m,k)} = \begin{cases} \frac{1}{\nu^k} \text{ST}(\tau_{ll'}^k + \nu^k (\hat{x}_l^{(m,k)} - \hat{x}_{l'}^{(m,k)}), \frac{\lambda_2}{\tau_2}), & \text{if } (l, l') \in \mathcal{E}^{(m-1)} \\ \hat{x}_{ll'}^{(m-1)}, & \text{if } (l, l') \notin \mathcal{E}^{(m-1)} \end{cases}. \quad (\text{A.10})$$

B Extension to Non-negative GRMF (N-GRMF)

B.1 Formulation for N-GRMF

In this section we show that our GRMF model can be easily extended to the robust non-negative MF with grouping effect (N-GRMF). The problem is formulated as follows

$$\min_{\mathbf{U} \in \mathbb{R}^{d \times r}, \mathbf{V} \in \mathbb{R}^{n \times r}} f(\mathbf{U}, \mathbf{V}) = \|\mathbf{Y} - \mathbf{U}\mathbf{V}^T\|_{\ell_1} + \mathcal{R}(\mathbf{U}) + \mathcal{R}(\mathbf{V}), \quad (\text{B.1})$$

where $\mathcal{R}(\mathbf{U})$ and $\mathcal{R}(\mathbf{V})$ are two regularizers corresponding to \mathbf{U} and \mathbf{V} , given by

$$\begin{aligned} \mathcal{R}(\mathbf{U}) &= \sum_{i=1}^d \lambda_1 \mathcal{P}_1(\mathbf{u}_i) + \sum_{i=1}^d \lambda_2 \mathcal{P}_2(\mathbf{u}_i) + \sum_{i=1}^d \lambda_3 \tilde{\mathcal{P}}_3(\mathbf{u}_i), \text{ and} \\ \mathcal{R}(\mathbf{V}) &= \sum_{j=1}^n \lambda_1 \mathcal{P}_1(\mathbf{v}_j) + \sum_{j=1}^n \lambda_2 \mathcal{P}_2(\mathbf{v}_j) + \sum_{j=1}^n \lambda_3 \tilde{\mathcal{P}}_3(\mathbf{v}_j). \end{aligned}$$

Here $\mathcal{P}_1(\cdot)$ and $\mathcal{P}_2(\cdot)$ are the same as in GRMF, while $\tilde{\mathcal{P}}_3(\cdot)$ is slightly different from $\mathcal{P}_3(\cdot)$, which takes the following form,

$$\mathcal{P}_1(\mathbf{x}) = \sum_{l=1}^r \min\left(\frac{|x_l|}{\tau_1}, 1\right), \quad \mathcal{P}_2(\mathbf{x}) = \sum_{l < l': (l, l') \in \mathcal{E}} \min\left(\frac{|x_l - x_{l'}|}{\tau_2}, 1\right), \quad \tilde{\mathcal{P}}_3(\mathbf{x}) = \sum_{l=1}^r (\min(x_l, 0))^2 \quad (\text{B.2})$$

We still adopt the ℓ_1 -loss to attain the robustness and solve the problem by fixing \mathbf{U} or \mathbf{V} and updating the other one.

B.2 Algorithms for N-GRMF

The solution for N-GRMF is very similar to that of GRMF. Thus, we will not walk through the whole solution here again. Instead, we only detail what differs in this model.

B.2.1 The DC algorithm

Note that in this model $\tilde{\mathcal{P}}_3(\mathbf{x})$ needs to be decomposed by DC just as $\mathcal{P}_1(\mathbf{x})$ and $\mathcal{P}_2(\mathbf{x})$ do. In particular, $S(\mathbf{x})$ can be decomposed as follows,

$$\begin{aligned} S_1(\mathbf{x}) &= \sum_{i=1}^n [(b_i - \mathbf{a}_i^T \mathbf{x})^2 + \epsilon]^{\frac{1}{2}} + \lambda_1 \sum_{l=1}^r \frac{|x_l|}{\tau_1} + \lambda_2 \sum_{l < l': (l, l') \in \mathcal{E}} \frac{|x_l - x_{l'}|}{\tau_2} + \lambda_3 \sum_{l=1}^r x_l^2 \\ S_2(\mathbf{x}) &= \lambda_1 \sum_{l=1}^r \left(\frac{|x_l|}{\tau_1} - 1\right)_+ + \lambda_2 \sum_{l < l': (l, l') \in \mathcal{E}} \left(\frac{|x_l - x_{l'}|}{\tau_2} - 1\right)_+ + \lambda_3 \sum_{l=1}^r [(x_l)_+]^2. \end{aligned}$$

For the m -th minimization, $S_2(\mathbf{x})$ is linearized and the subproblem becomes as follows,

$$S^{(m)}(\mathbf{x}) = \sum_{i=1}^n [(b_i - \mathbf{a}_i^T \mathbf{x})^2 + \epsilon]^{\frac{1}{2}} + \frac{\lambda_1}{\tau_1} \sum_{l \in \mathcal{F}^{(m-1)}} |x_l| + \frac{\lambda_2}{\tau_2} \sum_{l < l': (l, l') \in \mathcal{E}^{(m-1)}} |x_l - x_{l'}| + \lambda_3 \sum_{l \in \mathcal{N}^{(m-1)}} x_l^2, \quad (\text{B.3})$$

where

$$\begin{aligned} \mathcal{F}^{(m-1)} &= \left\{ l : |\hat{x}_l^{(m-1)}| < \tau_1 \right\}, \\ \mathcal{E}^{(m-1)} &= \left\{ (l, l') \in \mathcal{E}, |\hat{x}_l^{(m-1)} - \hat{x}_{l'}^{(m-1)}| < \tau_2 \right\}, \\ \mathcal{N}^{(m-1)} &= \left\{ l : \hat{x}_l^{(m-1)} < 0 \right\}. \end{aligned}$$

Denote $x_{ll'} = x_l - x_{l'}$, and define $\xi = (x_1, \dots, x_r, x_{12}, \dots, x_{1r}, \dots, x_{(r-1)r})$. The m -th subproblem (B.3) can be reformulated as an equality-constrained convex optimization problem,

$$S^{(m)}(\xi) = \sum_{i=1}^n [(b_i - \mathbf{a}_i^T \mathbf{x})^2 + \epsilon]^{\frac{1}{2}} + \frac{\lambda_1}{\tau_1} \sum_{l \in \mathcal{F}^{(m-1)}} |x_l| + \frac{\lambda_2}{\tau_2} \sum_{l < l' : (l, l') \in \mathcal{E}^{(m-1)}} |x_{ll'}| + \lambda_3 \sum_{l \in \mathcal{N}^{(m-1)}} x_l^2, \quad (\text{B.4})$$

subject to $x_{ll'} = x_l - x_{l'}$, $\forall l < l' : (l, l') \in \mathcal{E}^{(m-1)}$.

B.2.2 ADMM

The only thing different for N-GRMF in this step is the updating rule of $\hat{x}_l^{(m,k)}$, since \mathcal{P}_3 does not involve other variables but x_l . In particular, when updating by $\hat{x}_l^{(m,k)} = \alpha^{-1} \gamma$, α is a little different compared to the solution of GRMF and γ stays the same: it is formulated as follows,

$$\alpha = \sum_{i=1}^n D_i^{-\frac{1}{2}} A_{il}^2 + 2\lambda_3 I_{\{\hat{x}_l^{(m-1)} < 0\}} + \nu^k \left| l' : (l, l') \in \mathcal{E}^{(m-1)} \right|, \quad (\text{B.5})$$

where $I_{\{\hat{x}_l^{(m-1)} < 0\}} = 1$ when $\hat{x}_l^{(m-1)} < 0$ and $I_{\{\hat{x}_l^{(m-1)} < 0\}} = 0$ otherwise.

C More experiments

C.1 Additions to the main results

Figure 3 is a demonstration of the four datasets we used in the experiments. Each dataset consists of a large number of people or objects in different angles/expressions/light conditions. In this demonstration, the first row of images is the original version, and the second row of images is the corrupted version with 50% salt and pepper noise. In the experiment, we use each image as the input data, and then decompose it into two smaller matrices whose product constitutes the reconstructed image. We compare the reconstruction error between the original image and the reconstructed one.

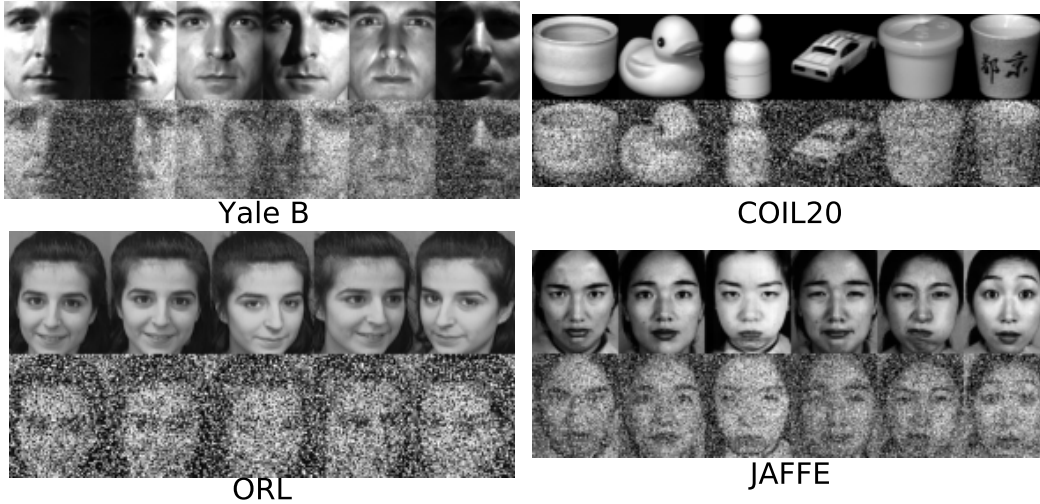


Figure 3: The original images and the corrupted versions. the first row of images is the original version, and the second row of images is the corrupted version with 50% salt and pepper noise.

Figure 4 shows one example of image recovery. The first column consists of input images with different corruption ratios. Each row represents the output images recovered by different methods. Among all methods, GRMF and PRMF demonstrate great recovery ability, especially when the corruption ratio is as high as 50%, where the output images look very similar to the original undamaged ones. Unlike these two, RPCA recovers the input image to the greatest extent, but it does not show robustness when the input image is corrupted with noise.

Table 3: Comparison of running time on the four datasets. The average time cost (seconds) per image is reported with the standard deviation in the parentheses. T-SVD stands for the Truncated SVD.

Datasets	Yale B		COIL		ORL		JAFPE	
	Origin	Corrupted	Origin	Corrupted	Origin	Corrupted	Origin	Corrupted
GRMF	155.7±(10.3)	334.6±(75.4)	188.4±(66.2)	480.7±(409.2)	85.1±(11.7)	159.2±(16.0)	177.4±(10.5)	353.4±(40.9)
PRMF	3.3±(0.1)	3.1±(0.1)	8.8±(20.3)	2.3±(0.6)	1.4±(0.1)	1.3±(0.0)	3.2±(0.1)	3.1±(0.2)
GMF-L2	27.2±(6.6)	20.6±(0.1)	42.0±(43.6)	22.5±(104.0)	21.3±(5.3)	9.0±(1.1)	22.5±(4.6)	18.1±(1.8)
GoDec+	0.1±(0.0)	0.0±(0.0)	0.1±(0.3)	0.0±(0.0)	0.0±(0.0)	0.0±(0.0)	0.0±(0.0)	0.0±(0.0)
T-SVD	0.0±(0.0)	0.0±(0.0)	0.0±(0.0)	0.0±(0.0)	0.0±(0.0)	0.0±(0.0)	0.0±(0.0)	0.0±(0.0)
RPCA	5.4±(0.1)	0.6±(0.1)	6.5±(12.9)	3.5±(0.4)	1.6±(0.1)	1.8±(0.1)	4.7±(0.1)	0.6±(0.1)
rNMF	0.5±(0.5)	5.1±(0.2)	6.5±(10.9)	3.0±(0.5)	1.7±(0.1)	1.8±(0.0)	4.5±(0.2)	4.5±(0.1)

As for the time cost, Table 3 demonstrates the average running time of different algorithms on the four datasets, including both the original version and the 50% corrupted version. Our algorithm is more time consuming compared to the benchmarks because we apply an algorithm which consists of multi-layer nested loops. To be specific, we update each row (column) of $U(V)$ independently, and each subproblem is solved with two nested loops combining DC and coordinate-wise ADMM. This structure is necessary in our approach because of the ℓ_0 -surrogate regularization and the grouping effect we are pursuing. The ℓ_0 -surrogate penalties are non-convex and thus can only be solved after decomposition into a difference of two convex functions. In addition, to pursue the grouping effect, we need to compare every pair of values in the output vector. Thus the resulting optimization problem could be solved by ADMM. In spite of that, the promoted performance of GRMF makes it worth being studied. The grouping effect of GRMF helps denoising the factorization and makes it less sensitive to outliers and corruption, which is demonstrated by the great recovery ability in the experiments of 50% corrupted images. Therefore, to enjoy the robustness and accuracy of GRMF, one significant future development of GRMF is to accelerate the training process.

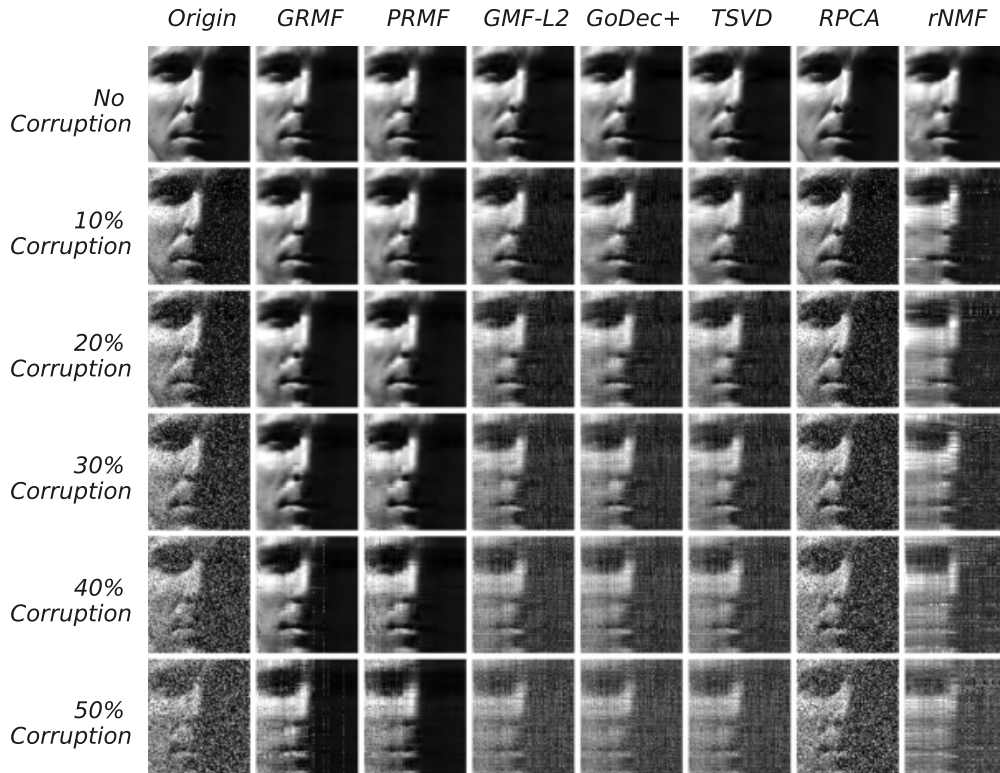


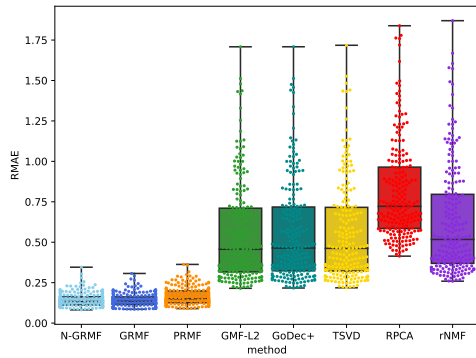
Figure 4: An example of image recovery with different MF methods under different corruption ratios.

Table 4: Comparison of Relative MAE among N-GRMF, regular GRMF, and PRMF on four datasets with 50% corruption ratio. The mean RMAE is reported with the standard deviation in the parentheses. N-GRMF stands for non-negative GRMF.

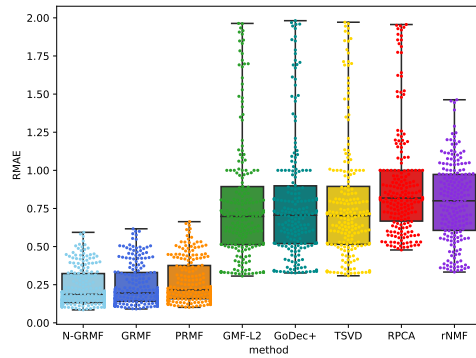
Datasets	Yale B		COIL		ORL		JAFFE	
	Origin	Corrupted	Origin	Corrupted	Origin	Corrupted	Origin	Corrupted
N-GRMF	0.093 \pm (0.022)	0.143 \pm (0.042)	0.123 \pm (0.066)	0.234 \pm (0.126)	0.105 \pm (0.020)	0.196 \pm (0.035)	0.121 \pm (0.013)	0.164 \pm (0.018)
GRMF	0.093 \pm (0.022)	0.143 \pm (0.041)	0.123 \pm (0.066)	0.245 \pm (0.135)	0.105 \pm (0.020)	0.204 \pm (0.036)	0.121 \pm (0.013)	0.165 \pm (0.018)
PRMF	0.095 \pm (0.023)	0.154 \pm (0.047)	0.127 \pm (0.070)	0.273 \pm (0.142)	0.107 \pm (0.020)	0.107 \pm (0.037)	0.125 \pm (0.014)	0.182 \pm (0.025)

C.2 Non-negative extension results

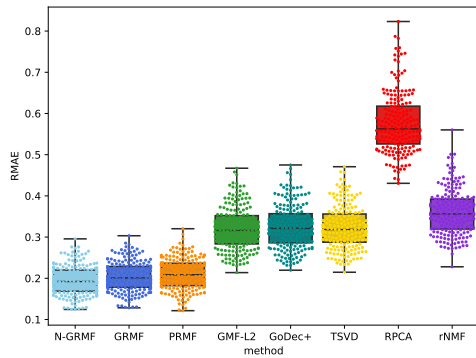
We extend our GRMF model to a non-negative variant (N-GRMF) and conduct matrix factorization using the same four datasets in this section. The algorithm of N-GRMF is covered in [Appendix B](#). Then [Table 4](#) demonstrates a comparison of the relative mean absolute error (RMAE) between non-negative GRMF, regular GRMF, and PRMF on four datasets with both its original version and the 50% corrupted version. The RMAE of GRMF and N-GRMF remains at the same level when doing factorization with respect to the origin image. Both GRMF and N-GRMF have a minor improvement on the corrupted image recovery. [Figure 5](#) illustrates the comparison of the reconstruction error between N-GRMF, regular GRMF, and all the benchmarks on four datasets with 50% corruption ratio. The distribution of the reconstruction error for each image is represented by the box plot and scatter plot, which shows the maximum, upper quantile, mean, standard deviation, lower quantile, minimum. Besides, every error point is plotted over it. As illustrated in [Table 4](#) and [Figure 5](#), the error of N-GRMF has a minor decrease compared with that of the regular GRMF without the non-negative constraint, when the input data is corrupted, implying an enhanced robustness from GRMF to N-GRMF.



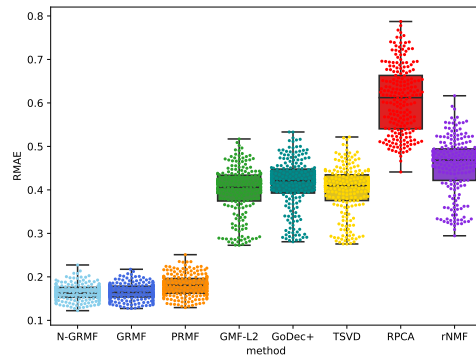
(a) RMAE of Yale B



(b) RMAE of COIL



(c) RMAE of ORL



(d) RMAE of JAFFE

Figure 5: Comparison of the distribution of relative mean absolute error(RMAE) among non-negative GRMF, regular GRMF, and all the benchmarks on four datasets with 50% corruption ratio. N-GRMF stands for non-negative GRMF, and T-SVD stands for the truncated SVD.